

Supplemental Information

Genome-scale sequencing and analysis of human, wolf and bison DNA from 25,000 year-old sediment

Pere Gelabert, Susanna Sawyer, Anders Bergström, Thomas C. Collin, Tengiz Meshveliani, Anna Belfer-Cohen, David Lordkipanidze, Nino Jakeli, Zinovi Matskevich, Guy Bar-Oz, Daniel M. Fernandes, Olivia Cheronet, Kadir T. Özdoğan, Victoria Oberreiter, Robin N. M. Feeney, Mareike C. Stahlschmidt, Pontus Skoglund, Ron Pinhasi

Figures S1 to S7

Tables S3 to S7

Figure S1. Sample descriptives: A) Metagenomic prediction with centrifuge, B), Length distribution of the four aligned mammalian species C) Deamination pattern of the filtered reads of the four mapped genomes: *Ovis aries*, *Homo sapiens*, *Bos taurus* and *Canis lupus*.

Figure S2. ADMIXTURE plots. ADMIXTURE plots using K from 1 to 15 of the human dataset.

Figure S3. f_3 -Outgroup analysis. A) Values of the f_3 -outgroup statistics in the combination $f_3(\text{SAT29}, X; \text{Mbuti})$. Only combinations with more than 2,000 SNPs were included, green dots represent post-LGM samples, violet dots represent pre-LGM samples and red dots represent farmer samples. Error bars denote standard errors. **B)** Results of the $f_3(\text{SAT29}, \text{Modern-population}; \text{Mbuti})$ combination.

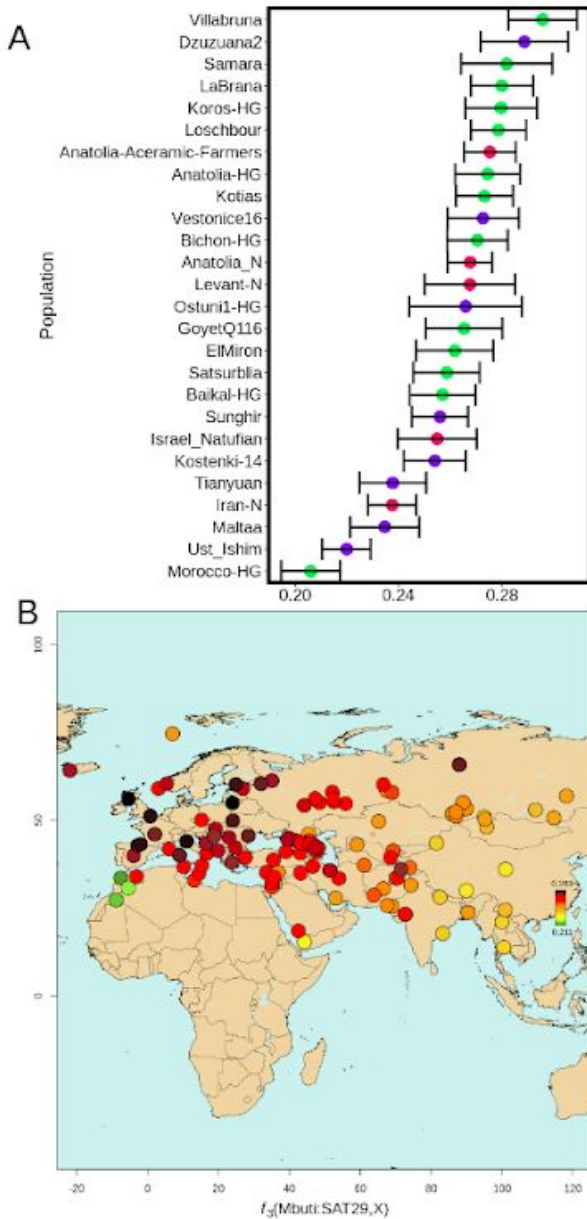


Figure S4. The SAT29 *Canis* genome is symmetrically related to modern wolves and dogs, and the latter share drift to the exclusion of SAT29. f_4 -statistics evaluating the basal ancestry status of the SAT29 canid genome in relation to a set of 15 diverse Eurasian present-day wolves and dogs. Error bars denote ± 3 standard errors. A) Statistics of the form $f_4(\text{CoyoteCalifornia}, \text{SAT29.Canis}; A, B)$ are consistent with being distributed around 0, indicating that SAT29 is symmetrically related to present-day individuals. A few statistics fall close to or slightly outside $|Z| > 3$ (largest $|Z| = 3.43$), and involve wolves from Southwestern and South Asia (WolfSyria, WolfSaudiArabia, Wolf07Israel, Wolf19India). However, the values of these statistics are in the direction of SAT29 being closer to other wolves than to these wolves, and thus likely reflects some basal ancestry in these present-day wolves, e.g. due to admixture from non-wolf canids. B) Statistics of the form $f_4(\text{CoyoteCalifornia}, A; B, \text{SAT29.Canis})$ are all negative, indicating that all of the present-day wolves and dogs share genetic drift that is not shared with the SAT29 sample.

Fig. S5. Principal component analysis on the *Ovis* and *Capra* dataset. The analysis was performed on a distance matrix comparing per-sample profiles of all possible f_4 -statistics of the form $f_4(X,A;B,C)$ where X is the focal sample.. S12: PC 1-2 plot, S13: PC 3-4 plot, S14: PC 5-6 plot, S15: PC 7-8 plot, S16: PC 9-10 plot.

Figure S6. Two microphotographs (A, B) from block sample SAT 15 14. The microphotographs were taken adjacent to SAT 16 LS29, in cross- (XPL) and plane-polarized light (PPL), showing dominant components and processes. Typical anthropogenic components are bone (B), burnt bone (BB), charcoal (Ch) and flint (Fl). Note also the occurrence of rounded soil aggregates (yellow circles) that were transported into the cave from soils forming outside and that exhibit cross-striations of the clay component resulting from repeated wetting and drying cycles during their formation. Similarly, clay coatings in voids (blue arrow) result from water percolating through the sediment.

Figure S7. Evidence for polymorphism in the SAT29 wolf mitochondrial sequence.

Sites that differ between the pre-LGM Armenian wolf TU10 and the major clade of wolf mitochondria were identified, and the read counts of the SAT29 sample at these sites displayed. Dark blue indicates SAT29 reads matching the major clade allele, while light blue indicates SAT29 matching the TU10 allele. Variants are stratified by mutational direction, with sites where derived mutations in SAT29 and TU10 can not be explained by C->T deamination on the left (black text), and sites where they could be on the right (gray text). A) Results for all reads. B) Results restricted to reads displaying evidence of deamination. These results suggest that the retrieved DNA derives from more than one wolf individual.

Table S3. Human Mitochondria derived positions: Derived positions of the SAT29 mitochondrial genome respect the rCRS sequence. Bold positions are the ones that have been accepted because the ratio derived/no derived was higher than 2%.

Position	Coverage	Alleles	Haplogroup
73	7	0 A / 7 G	N
263	24	2 A / 22 G	N
750	22	A 0 / G 22	N
1438	9	A 0 / G 9	N
2706	8	A 1 / G 7	N
4769	12	A 1 / G 11	N
7028	15	1 C / 14 T	N
8860	12	1 A / 11 G	N
11719	14	0 G / 14 A	N
12705	12	2 C / 10 T	N
14766	20	0 C / 20 T	N
15326	17	0 A / 17 G	N
16223	16	7 C / 9 T	N
152	5	2 T / 3 C	private
827	13	7 A / 6 G	private
8655	14	4 C / 10 T	private
12451	15	6 A / 9 G	private
12662	19	A 6 / 13 G	private
14218	17	5 T / 12 C	private
16189	14	7T/7C	private
16519	8	0 T / 8 C	hotspot

Table S6. f_4 -outgroup statistics results of SAT29 with human ancient individuals: f_4 -statistics results in the combination $f_4(\text{Dzuzuana2}, X; \text{SAT29}, \text{Mbuti})$.

Pop A	Pop B	Pop C	Pop D	f_4 -value	SD	Z score	SNPs
Dzuzuana2	Anatolia_N	SAT29	Mbuti	0.007312	0.003279	2.230	4463
Dzuzuana2	Tianyuan	SAT29	Mbuti	0.010573	0.004824	2.192	3673
Dzuzuana2	Vestonice16	SAT29	Mbuti	0.009875	0.005098	1.937	3118
Dzuzuana2	Kotias	SAT29	Mbuti	0.007575	0.004297	1.763	4483
Dzuzuana2	Satsurblia	SAT29	Mbuti	0.005941	0.005189	1.145	3198
Dzuzuana2	GoyetQ116	SAT29	Mbuti	0.010481	0.005157	2.032	3240
Dzuzuana2	Koros-HG	SAT29	Mbuti	-0.000125	0.004673	-0.027	3327
Dzuzuana2	ElMiron	SAT29	Mbuti	-0.002115	0.005708	-0.371	2659
Dzuzuana2	LaBrana	SAT29	Mbuti	0.003839	0.004445	0.864	4222
Dzuzuana2	Iran-N	SAT29	Mbuti	0.010591	0.003743	2.830	4285
Dzuzuana2	Villabruna	SAT29	Mbuti	-0.004202	0.004553	-0.29	1954
Dzuzuana2	Ostuni1-HG	SAT29	Mbuti	-0.001887	0.007509	-0.251	1369
Dzuzuana2	Levant-N	SAT29	Mbuti	0.003945	0.013064	0.30	507
Dzuzuana2	Loschbour	SAT29	Mbuti	0.003366	0.003852	0.874	4438
Dzuzuana2	Morocco-HG	SAT29	Mbuti	0.019854	0.004474	4.438	4021
Dzuzuana2	Samara	SAT29	Mbuti	0.005471	0.006641	0.824	2003
Dzuzuana2	Kostenki-14	SAT29	Mbuti	0.004512	0.004462	1.011	4257
Dzuzuana2	Maltaa	SAT29	Mbuti	0.011467	0.005187	2.211	4257
Dzuzuana2	Sunghir	SAT29	Mbuti	0.009413	0.004071	2.312	4484
Dzuzuana2	Ust_Ishim	SAT29	Mbuti	0.015006	0.003692	4.065	4476
Dzuzuana2	Bichon-HG	SAT29	Mbuti	0.004794	0.004296	1.116	4476
Dzuzuana2	Baikal-HG	SAT29	Mbuti	0.002936	0.004688	0.626	3562
	Anatolia-Acerami						
Dzuzuana2	c-Farmers	SAT29	Mbuti	0.005734	0.003898	1.471	4272
Dzuzuana2	Anatolia-HG	SAT29	Mbuti	0.007690	0.004857	1.583	3484
Dzuzuana2	Israel_Natufian	SAT29	Mbuti	0.004809	0.005557	0.865	2411

Table S7. Human mitochondrial mapping differences: Mitochondrial mapping differences between the three different bins: A) All reads, B) Deaminated reads, C) Non deaminated reads. The discordant positions are shown in this table

Positions	All Reads	Non deaminated reads	Deaminated reads
497	7C/6T	1T/3C	2T/1C
3480	5G/5A	5G/1A	3A
11914	11G/3A	2G/3A	7G
14905	9G/8A	4G/7A	4G